Supplementary Information

A Sensitive, Selective Electrochemical Detection and Kinetic Analysis of Methyl Parathion over Au Nanoparticles Decorated rGO/CuO Ternary Nanocomposite

N. I. Nayem[a], M. Sabbir Hossain[a], Md. A. Rashed[a*], K. M. Anis-Ul-Haque[b], Jahir Ahmed[c,d], M. Faisal[c,d], Jari S. Algethami[c,d], Farid A. Harraz[c,e*]

[a] Department of Chemistry, Faculty of Science, Mawlana Bhashani Science and Technology University, Santosh, Tangail-1902, Bangladesh

[b] Department of Chemistry, Jessore University of Science and Technology, Jessore-7408, Bangladesh

[c] Advanced Materials and Nano-Research Centre (AMNRC), Najran University, Najran 11001, Saudi Arabia

[d] Department of Chemistry, Faculty of Science and Arts, Najran University, Najran 11001, Saudi Arabia

[e] Department of Chemistry, Faculty of Science and Arts at Sharurah, Najran University, Sharurah 68342, Saudi Arabia

[*] **Corresponding authors:**

E. mail: rashedlizon@gmail.com; abu.rashed@mbstu.ac.bd (Md. A. Rashed)

E. mail: faharraz@nu.edu.sa (Farid A. Harraz)

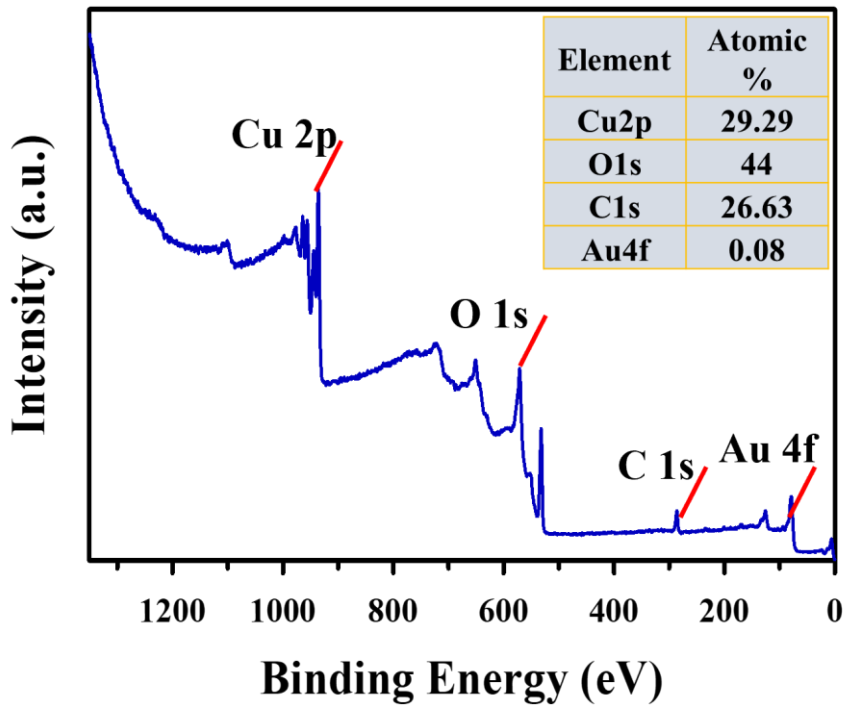

Fig. S1 XPS survey scan spectra of Au@rGO/CuO. Inset depicts elemental composition (At%).

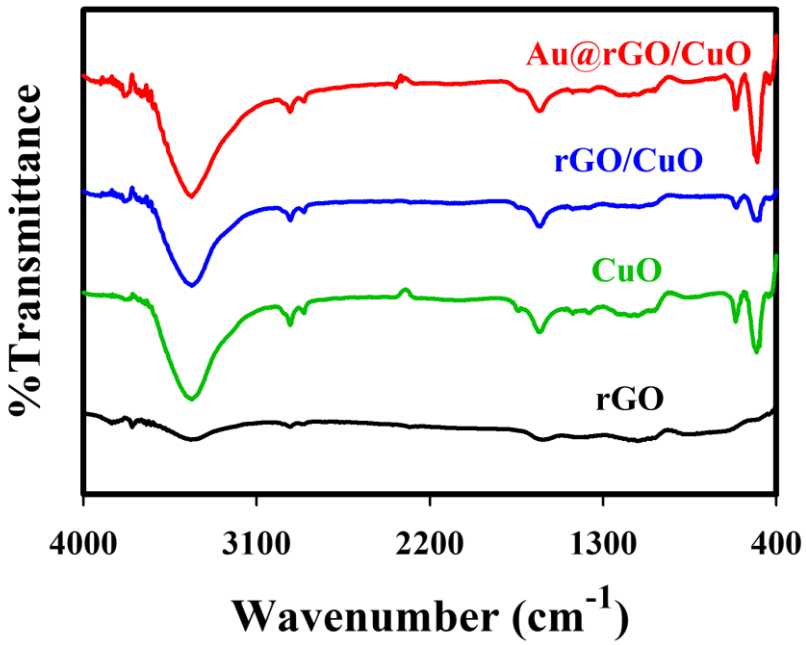

Fig. S2 FTIR spectra of rGO, CuO, rGO/CuO and Au@rGO/CuO nanocomposite.

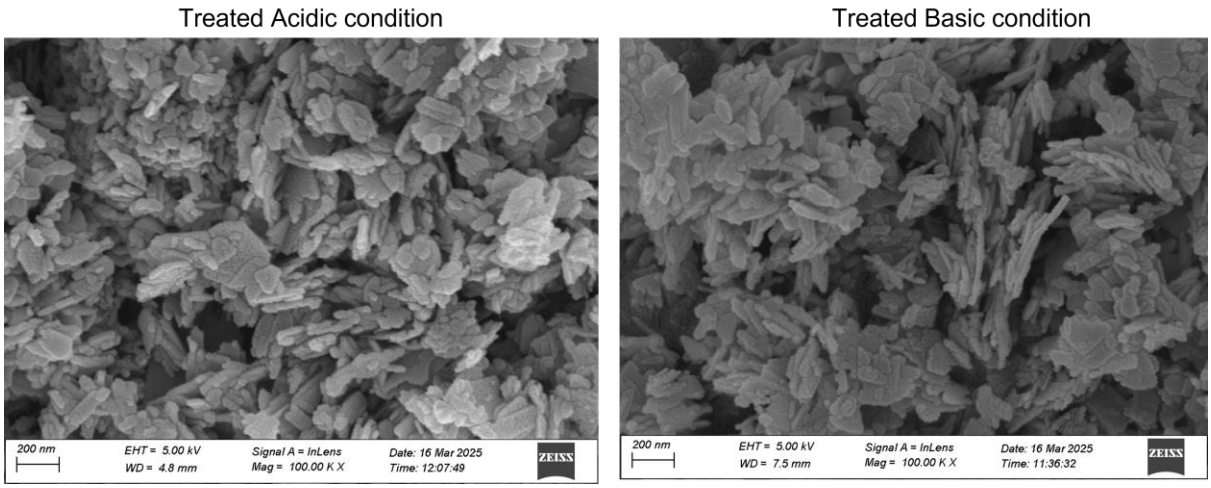

Fig. S3 FESEM images of 1M HCl and 1M NaOH treated as-fabricated Au@rGO/CuO nanocomposite.

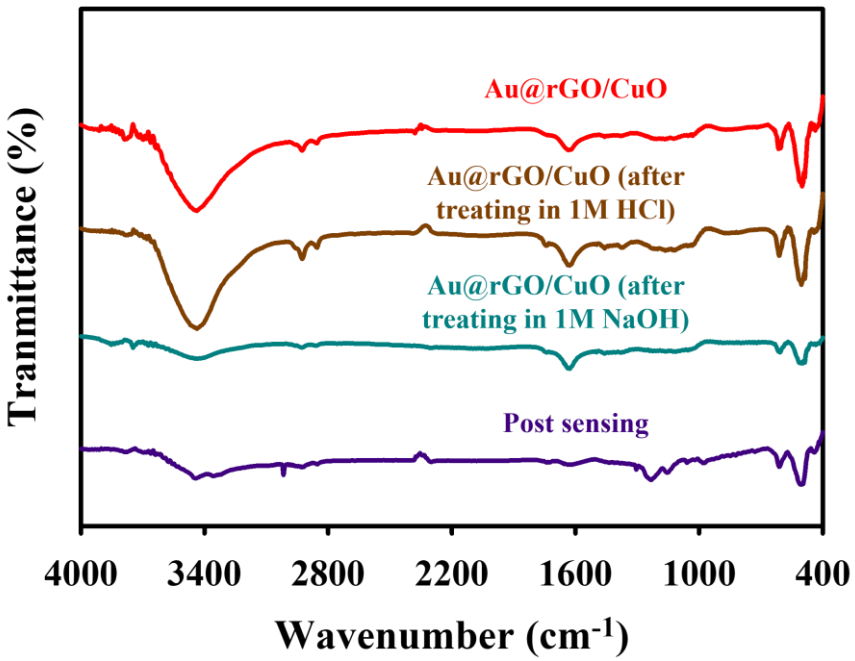

Fig. S4 FTIR spectra of Au@rGO/CuO pre-sensing, expose to harsh conditions (1M HCl and 1M NaOH for three days), and post-sensing conditions.

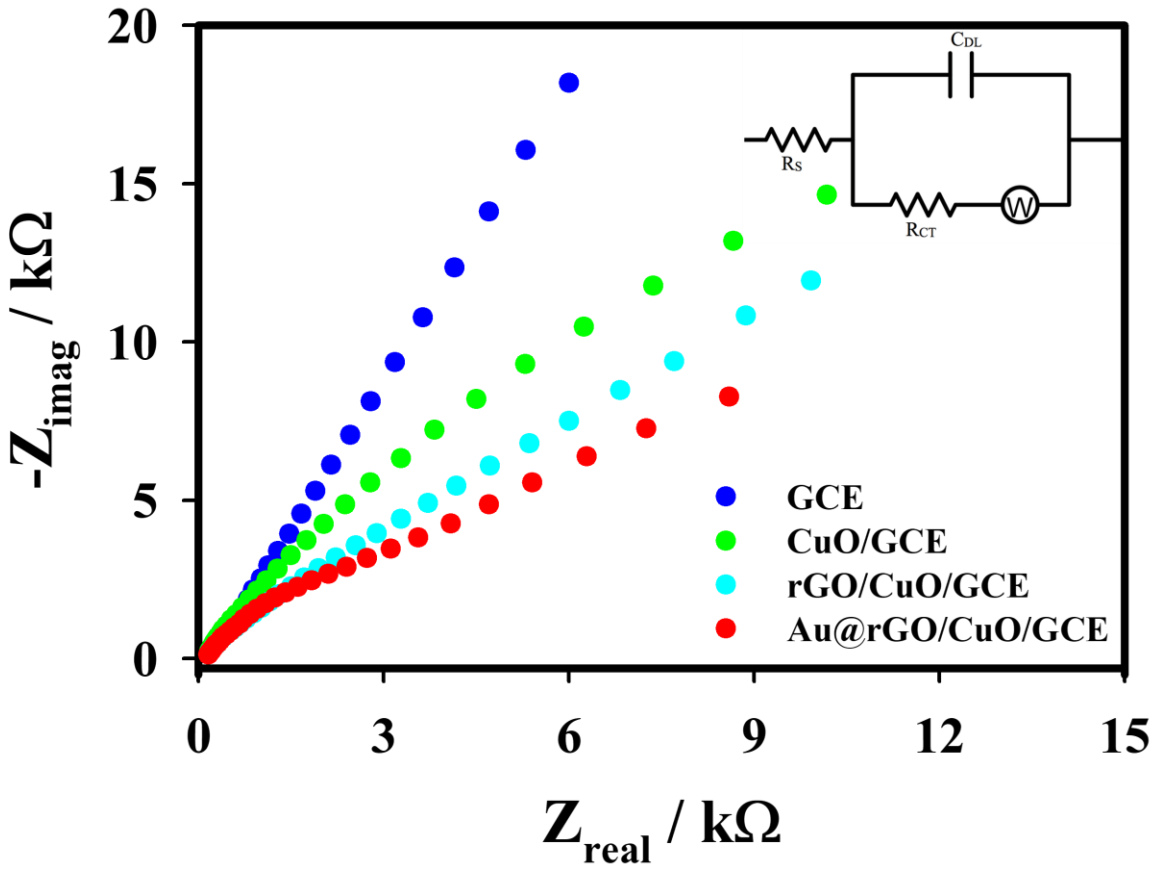

Fig. S5 EIS Nyquist response for bare GCE, CuO/GCE, rGO@CuO/GCE, and Au@rGO/CuO/GCE in 0.1 M PBS (pH = 7.0) containing 30 μM of MP, working electrodes in conditions: 1 to 10^3 Hz frequency and signal amplitude $= 0.05\,V$ with applied potential $-0.6\,V$ vs. Ag/AgCl (KCl). Inset shows the Randless equivalent circuit.

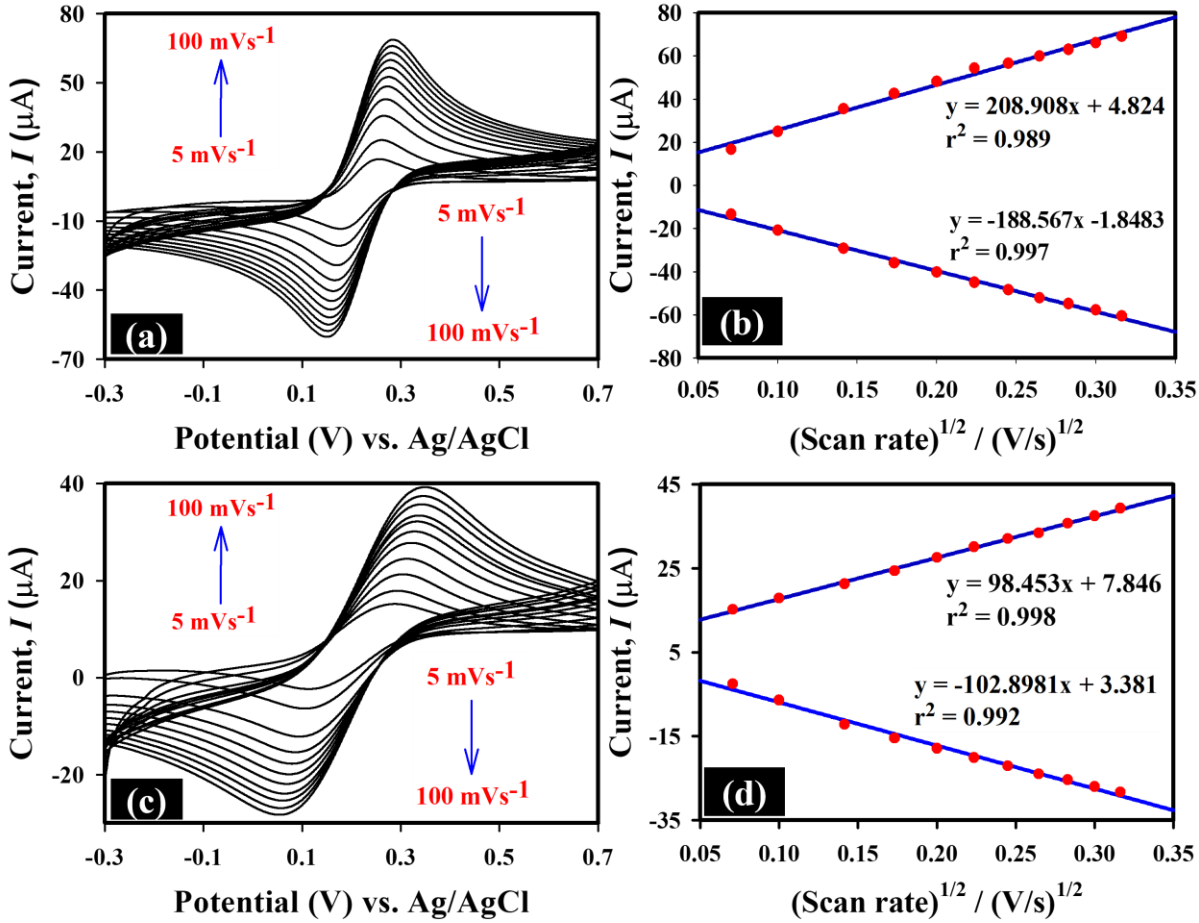

Fig. S6 Cyclic voltammograms recorded in 3.0 mM $K_3Fe(CN)_6$ + 0.1 M KCl with the variation of scan rate using (a) Au@rGO/CuO/GCE and (c) unmodified GCE. Plot of anodic and cathodic peak current *vs*. sq. root of scan rate for (b) Au@rGO/CuO/GCE and (d) unmodified GC electrodes.

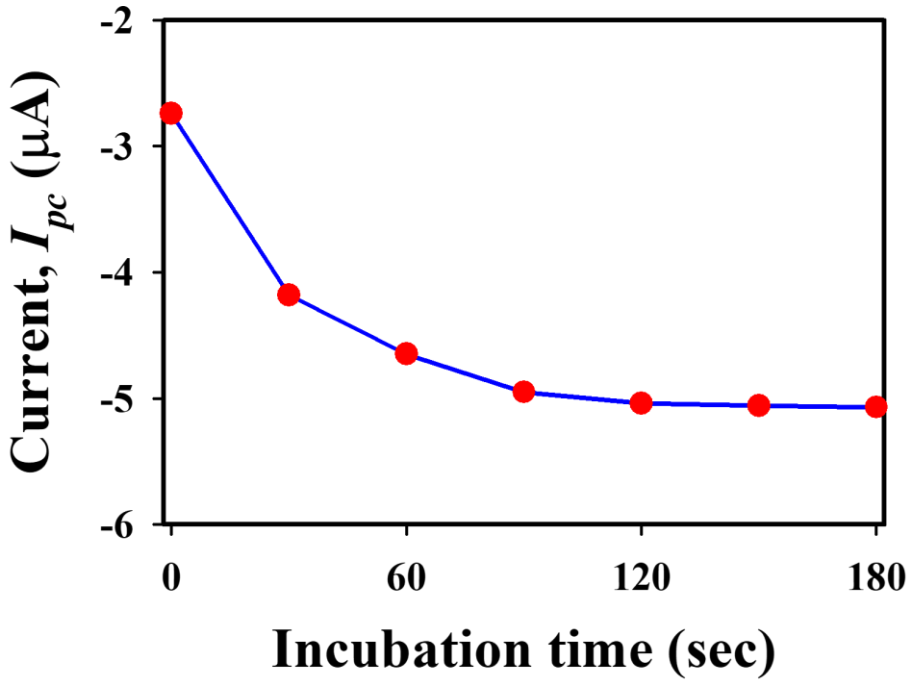

Fig. S7 Effect of accumulation time on the cathodic current response studied by SWV in 10 μ*M* MP in 0.1 *M* PBS at pH= 7.0.

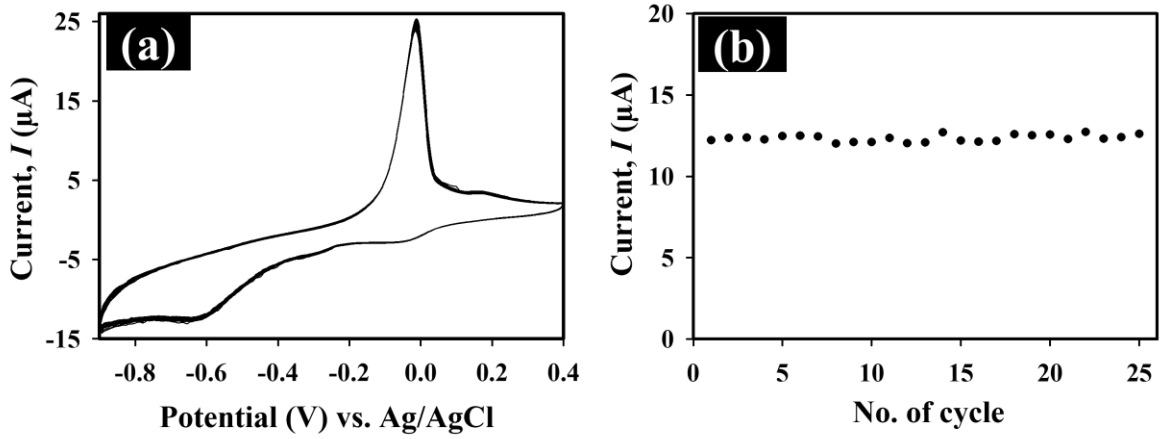

Fig. S8 (a) CV response of Au@rGO/CuO/GCE electrode in 25 consecutive cycles measured in 30 µ$M\ MP\ +\ 0.1\ M\ PBS$ (pH= 7.0) with a scan rate 50 mVs^{-1}, (b) shows the current intensity with respect to the number of repeated cycles.

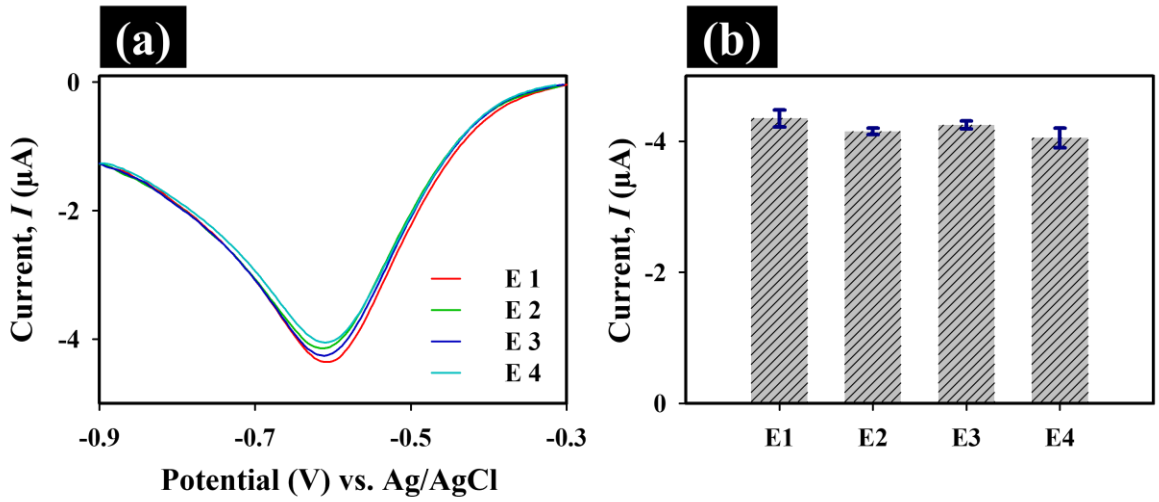

Fig. S9 (a) Reproducibility was checked by SWV in four different Au@rGO/CuO/GCE electrodes in 10 μM MP in 0.1 M PBS at pH= 7.0. (b) Bar diagram of current intensity *vs.* number of electrodes.

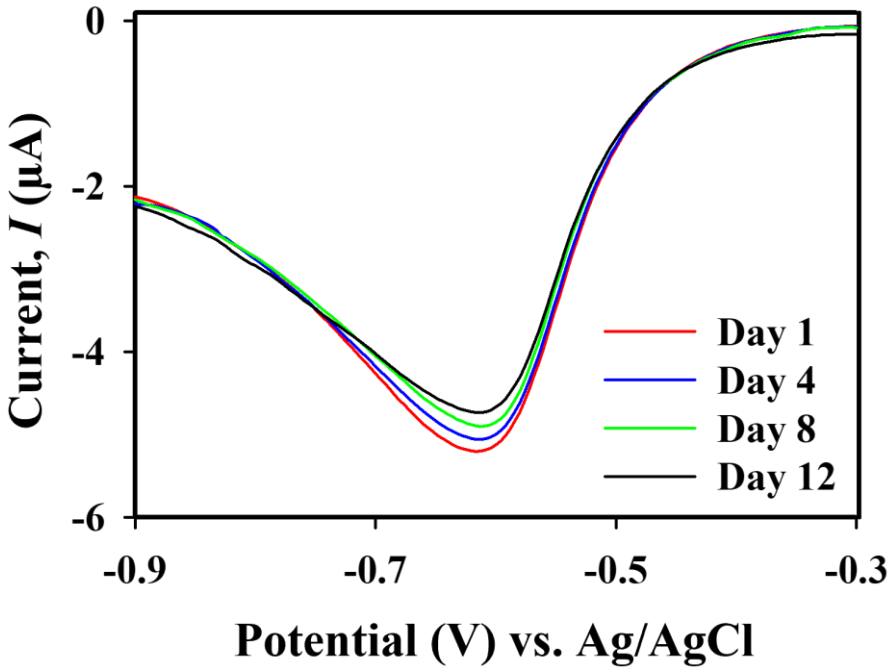

Fig. S10 Storage stability test using SWV response recorded with 10 μM MP in 0.1 M PBS (pH= 7.0).

Table S1: Recovery results of MP in surface water samples using the SWV approach via the standard addition procedure.

Real sample (River Water)	MP Added (µM)	MP Found (µM)	Recovery (%)	% RSD
Bangshi river	15	15.2	101.33	1.31
		14.9	99.33	
		14.83	98.86	
	20	19.2	96.03	2.55
		20.2	101.08	
		19.63	98.16	
	30	30.3	101.0	2.57
		28.9	96.3	
		29.1	96.9	
Dhaleshwari river	15	14.78	98.53	1.39
		14.85	99	
		15.17	101.13	
	20	19.36	96.84	3.54
		20.23	101.26	
		20.77	103.88	
	30	29.8	99.22	1.97
		30.4	101.44	
		31.0	103.22	